Nickel(II) and manganese(II) complexes of substituted phenanthroline ligands

Md. Athar Masood and Derek J. Hodgson*
Department of Chemistry, University of Wyoming, Laramie, WY 82071 (USA)

P.S. Zacharias*
School of Chemistry, University of Hyderabad, Hyderabad 500 134 (India)

(Received November 25, 1993; revised February 8, 1994)

Abstract

The synthesis and characterization of nickel(II) and manganese(II) complexes of substituted 1,10-phenanthroline ligands are described.; The ligands include 2,9-di(*o*-tolyl)-1,10-phen (dtphen), 2,9-di(2-methoxyphenyl)-1,10-phen (dmophen), 2,9-di(2-ethoxyphenyl)-1,10-phen (deophen), 2-(*o*-tolyl)-1,10-phen (tphen), 2-(2-ethoxyphenyl)-1,10-phen (eophen) and 2,9-bis(*N*-pyrazolylmethyl)1,10-phen (bpmp). 1:1 Metal-to-ligand complexes have been isolated with dmophen and bpmp, and 1:2 metal-to-ligand complexes have been isolated with all ligands except bpmp. The structure of 1:1 nickel(II) complex with dmophen has been determined by three-dimensional X-ray diffraction methods. The complex [Ni(dmophen)Cl_2], [$NiC_{26}H_{20}N_2O_2Cl_2$], crystallizes in the space group *Pccn* of the orthorhombic system with eight molecules in a cell of dimensions $a = 14.572(3)$, $b = 16.741(3)$ and $c = 19.209(4)$ Å. The structure has been refined to a final value of the crystallographic R factor of 0.0427 based on 2618 observed independent reflections. There are two crystallographically independent, but geometrically very similar, molecules in the cell, each lying on a twofold axis. The complex is roughly tetrahedral, the coordination being provided by two ligand phen nitrogen atoms and by two chloride ions. Electrochemical data for the 1:2 complexes suggest that the M(II) ↔ M(I) electron transfer process is essentially metal localized, but that the M(I) ↔ M(0) electron transfer process is ligand localized. Moreover, the electrochemical results demonstrate that the 2,9-di(*o*-substituted phenyl)-1,10-phen ligands are able to stabilize lower oxidation states, and that ligand binding to the reduced metal ion prevents its dissociation into free ligand and metal.

Key words: Crystal structures; Nickel complexes; Manganese complexes; Phenanthroline complexes

Introduction

We have recently reported new sets of related ligands, 2,9-di(*o*-substituted phenyl)-, 2,9-bis(*N*-pyrazolylmethyl)- and 2-(*o*-substituted phenyl)-1,10-phenanthrolines [1, 2]. The phenyl substituted ligands of phen form complexes with two ligands enclosing the metal ion to provide an M(N-N)$_2$ chromophore while the 2,9-bis(*N*-pyrazolylmethyl)-1,10-phen ligand forms 1:1 pseudo-octahedral complexes with four ligand nitrogen donors and two water (or other solvent) molecules. The ligands which have bulky (*o*-substituted phenyl) groups at the 2 and 9 positions of phen bring about strong steric interactions leading to distorted tetrahedral geometries [2, 3]. The aromatic character of the ligands, combined with their strong π-accepting ability resulting from the low-lying π^* orbitals of the phen units and with the steric interactions caused by *o*-substituted alkoxyphenyl groups, help to stabilize complexes in which the metal is in lower formal oxidation states. On the other hand, the five-membered heterocyclic rings are much poorer π acceptors (and better π donors), and since the 2,9-bis(*N*-pyrazolylmethyl)phen ligand contains both these soft and hard sites, unusual electrochemical behavior of their metal complexes could be anticipated.

Numerous nickel complexes of phenanthroline and substituted phenanthroline ligands are documented, but examples of lower oxidation state metal complexes with nitrogen donors are restricted to tetraaza macrocyclic ligands [4], quinquedentate ligands [5] and a recently reported nickel catenate [6]. Stability of the nickel(I) oxidation state (real or formal) is either the result of the macrocyclic effect or the topological effect [7, 8]

*Authors to whom correspondence should be addressed.

SSDI 0020-1693(94)03961-M

of the cyclic ligands and tetrahedral/distorted tetrahedral is the preferred geometry in this oxidation state. Such an arrangement disfavors the +2 oxidation state, since the affinity of nickel(II) for such (hypothetical) ligands is too low, precluding the preparation and characterization of the corresponding complexes.

With regard to manganese, those complexes which are multinuclear and have high oxidation states show quasi-reversible or reversible behavior with the redox waves corresponding to the IV/IV↔IV/III and IV/III↔III/III couples [9, 10], but here too where macrocycles are present, the reversibility is more pronounced due to macrocyclic effect [11]. Mononuclear complexes of manganese(II), however, simply show irreversible behavior [12, 13], while some of the mononuclear manganese(III) complexes do undergo reversible redox cycles involving higher oxidation states [14].

In view of these earlier observations, it seemed appropriate to study the manganese and nickel complexes of the present ligands which are expected to favor tetrahedral/pseudo-tetrahedral and octahedral geometrics, and compare their electrochemical propertics with each other and with those of other related species. This would also allow the study of the extent of stabilization of the M(I) and M(0) complex species, if generated.

Experimental

Materials

All solvents were of reagent grade and distilled either over CaH_2 or Na wire and stored over molecular sieve prior to use. The starting materials were either purchased (Merck, Fluka or Aldrich) or prepared as indicated below.

Preparation of the ligands

The ligands 2,9-di(*o*-tolyl)-1,10-phen (dtphen), 2,9-di(2-methoxyphenyl)-1,10-phen (dmophen), 2,9-di(2-ethoxyphenyl)-1,10-phen (deophen), 2-(*o*-tolyl)-1,10-phen (tphen), 2-(2-ethoxyphenyl)-1,10-phen (eophen) and 2,9-bis(*N*-pyrazolylmethyl)-1,10-phen (bpmp) were prepared as described earlier [1, 2].

Caution. Although the prcparations of the perchlorate salts described here have been carried out without incident, perchlorate salts of metal complexes with organic ligands have been known to explode spontaneously. Therefore, preparation and handling of these perchlorate salts deserve special care.

Preparation of the 1:1 ligand to metal complexes

To the bpmp ligand (1.1 mmol) dissolved in CH_2Cl_2–MeOH (1: vol./vol., 10 ml) was added a 5 ml methanolic solution of $Mn(ClO_4)_2 \cdot 6H_2O$ or $Ni(ClO_4)_2 \cdot 6H_2O$ (1 mmol) with stirring. In the case of manganese the solution turned light yellow while in the case of nickel it turned light yellowish green. For the manganese complex, when the volume of the solution was reduced to half, a light yellow solid precipitated; this was filtered and washed with 1 ml of MeOH and 25 ml of ether. In the case of nickel, the solution was evaporated and 5 ml acetonitrile was added to give a deep purple solution. On passage of ether vapors into the solution, a purple solid was deposited which was found to lose its solvent of crystallization very quickly to give a violet powder.

The complex $[Ni(dmophen)Cl_2]$ was prepared analogously by reacting 1 mmol dmophen ligand with 1 mmol $NiCl_2 \cdot 6H_2O$ to give a dark yellowish brown solid.

Preparation of the 2:1 ligand to metal complexes

To the appropriate ligand (except bpmp) (2.1 mmol) dissolved in CH_2Cl_2–MeOH (1:1 vol./vol., 5 ml) was added a 5 ml methanolic solution of $Mn(ClO_4)_2 \cdot 6H_2O$ or $Ni(ClO_4)_2 \cdot 6H_2O$ (1 mmol) with stirring. A light green solution resulted in the case of nickel and a light yellow solution resulted in the case of manganese; on heating for 5 min, the latter turned a little darker in color. When the volume of the solution was reduced to half, light yellowish green (nickel) or light yellow (manganese) solids precipitated.

Physical measurements

The analyses of C, H and N were carried out on a Perkin-Elmer 240C analyzer. Conductivity measurements were performed on a CM-82T Elico conductivity meter at 25 °C in nitromethane at a concentration of 0.001 mol dm^{-3}. IR spectra were recorded on a Perkin-Elmer IR 283 spectrophotometer or a Perkin-Elmer 1600 FT-IR spectrophotometer. Magnetic susceptibilities were determined on a Brucker BM6 magnet with a Faraday magnetic balance using $HgCo(SCN)_4$ as the calibrant. Electronic spectra were obtained by using 2×10^{-3} mol dm^{-3} solutions in MeCN for the visible range and 1×10^{-5} mol dm^{-3} solutions for the UV range in case of phenyl substituted ligands, while in the case of the bpmp complexes the MeCN solutions were 1×10^{-3} mol dm^{-3} for the UV range. They were recorded either on a Perkin-Elmer Lambda 3B UV–Vis spectrophotometer or Perkin-Elmer Lambda 9 spectrophotometer. Cyclic voltammetry (CV) and differential pulse voltammetry (DPV) experiments were carried out either on a PAR electrochemistry system consisting of a 174A polarographic analyzer and a single compartment cell or a BAS 100A electrochemical analyzer. Solutions of the complexes were approximately 1×10^{-3} mol dm^{-3} in MeCN. The supporting electrolyte was 0.1 mol dm^{-3} tetraethylammonium perchlorate. For the PAR instrument, the working electrode was a hanging mercury drop electrode, the auxiliary electrode was a coiled

platinum wire and the reference electrode was a saturated calomel electrode (SCE). For the BAS instrument, the working electrode was glassy carbon and the reference electrode was Ag/AgCl. The experiments are uncorrected for liquid junction potential and were performed under a blanket of dry nitrogen at 25 ± 1 °C. With the exception of the nickel(II) complex of dmophen, efforts to grow crystals of the complexes described above were unfruitful; in some cases crystalline material which did not diffract was obtained, and in others the complex evidently instantaneously loses solvent of crystallization, forming a powder.

X-ray crystallography

X-ray quality crystals of [Ni(dmophen)Cl_2] were grown from acetonitrile solutions to give yellow–brown rectangular plate-shaped crystals. The structure of the complex was determined at 22 °C (295 K) on a Nicolet R3m/V diffractometer equipped with a molybdenum tube ($\lambda(K\alpha_1) = 0.70926$, $\lambda(K\alpha_2) = 0.71354$ Å) and graphite monochromator. The structure was solved by direct methods and refined by least-squares techniques, the programs being from the SHELXTL IRIS system. The data were corrected for Lorentz–polarization and for absorption effects. Crystallographic details and cell constants are found in Table 1.

A crystal of dimensions 0.80 × 0.60 × 0.40 mm was mounted. Data were collected in the range $4 \leqslant 2\theta \leqslant 55°$, with $0 \leqslant h \leqslant 18$, $-21 \leqslant k \leqslant 0$, $0 \leqslant l \leqslant 24$. All hydrogen atoms were placed in fixed calculated positions (C–H = 0.96 Å). All non-hydrogen atoms were refined anisotropically. Final values of the conventional R factors were $R = 0.0427$ and $R_w = 0.0679$ based on 2618 independent data with $F \geqslant 6\sigma(F)$. Final atomic positional parameters and their estimated standard deviations are presented in Table 2.

TABLE 1. Crystallographic data for the complex

Formula	$[C_{26}H_{20}Cl_2N_2NiO_2]$
Color; habit	green–brown; rectangular plate
a (Å)	14.572(3)
b (Å)	16.741(3)
c (Å)	19.209(4)
V (Å^3)	4686(2)
Z	8
FW	522.0
Space group	$Pccn$
T (°C)	22
ρ_{calc} (g cm^{-3})	1.480
μ (mm^{-1})	1.033
NO[a]	5387
$NO(F > 6\sigma(F))$	2618
R[b]	0.0427
R_w[c]	0.0679

[a]NO = no. of observed reflections. [b]$R = \Sigma||F_o| - |F_c||/\Sigma|F_o|$. [c]$R_w = [\Sigma w(|F_o| - |F_c|)^2/\Sigma w|F_o|^2]^{1/2}$.

TABLE 2. Atomic coordinates (× 10^4) and equivalent isotropic displacement coefficients (Å^2 × 10^3) for $C_{26}H_{20}Cl_2N_2NiO_2$

	x	y	z	U_{eq}[a]
Ni(1)	7500	7500	4703(1)	42(1)
Ni(2)	7500	2500	2997(1)	43(1)
N(1)	7482(3)	8301(2)	3920(2)	40(1)
N(2)	8267(3)	2068(2)	3782(2)	43(1)
Cl(1)	6126(1)	7700(1)	5143(1)	97(1)
Cl(2)	7020(1)	1378(1)	2512(1)	60(1)
O(1)	6106(3)	10223(2)	4280(2)	64(1)
O(2)	9517(3)	83(3)	3327(3)	89(2)
C(1)	7425(4)	9101(3)	3940(3)	44(1)
C(2)	7410(4)	9549(3)	3330(3)	50(2)
C(3)	7435(4)	9186(3)	2698(3)	55(2)
C(4)	7477(4)	8347(3)	2659(3)	55(2)
C(5)	7489(5)	7905(4)	2022(3)	72(2)
C(6)	7494(3)	7933(3)	3298(2)	43(1)
C(7)	7409(4)	9491(3)	4631(3)	45(2)
C(8)	6742(4)	10082(3)	4789(3)	49(2)
C(9)	6744(5)	10441(3)	5434(3)	61(2)
C(10)	7405(5)	10246(3)	5914(3)	64(2)
C(11)	8055(5)	9689(3)	5769(3)	64(2)
C(12)	8059(4)	9314(3)	5131(3)	50(2)
C(13)	5483(5)	10877(4)	4372(4)	83(3)
C(14)	9010(4)	1601(3)	3754(3)	53(2)
C(15)	9398(5)	1293(4)	4377(4)	70(2)
C(16)	9052(5)	1498(4)	4990(4)	75(3)
C(17)	8292(4)	2006(4)	5041(3)	61(2)
C(18)	7856(5)	2267(4)	5678(3)	76(3)
C(19)	7905(4)	2261(3)	4404(3)	49(2)
C(20)	9421(4)	1443(3)	3069(3)	58(2)
C(21)	9675(4)	678(4)	2849(4)	73(2)
C(22)	10023(5)	558(5)	2201(5)	93(3)
C(23)	10143(5)	1192(6)	1747(4)	89(3)
C(24)	9933(5)	1951(5)	1956(4)	84(3)
C(25)	9589(4)	2082(4)	2618(3)	68(2)
C(26)	9749(6)	−709(5)	3158(6)	114(4)

[a]Equivalent isotropic U defined as one third of the trace of the orthogonalized U_{ij} tensor.

Results and discussion

The complexes were characterized by analytical and spectral methods and the data are tabulated in Table 3. Except for the bpmp ligand, all other ligands form complexes with a 1:2 metal to ligand ratio while bpmp forms complexes with a 1:1 metal to ligand ratio. All the complexes exhibit a strong and broad IR peak, the center of which is located at about 1090 cm^{-1}, and a single sharp peak near 620 cm^{-1}. This latter band is characteristic of ionic perchlorate [15a]. The IR spectra do not exhibit a broad band at 250 to 300 cm^{-1}, which indicates the bis chelate nature of the complexes [15b]. The other IR bands are consistent with the presence of coordinated phen ligands. The IR spectra of manganese and nickel bpmp complexes are virtually identical and also have bands at about 3400 cm^{-1} due to water

TABLE 3. Analytical and physical data for the complexes

Complex	Elemental analysis (%)[a]			Conductance (Ω^{-1} cm^2 mol^{-1})	λ_{max} (nm) (log ϵ)	Magnetic moment, μ_B
	C	H	N			
$[Ni(dtphen)_2]^{2+}$	63.57 (63.82)	4.01 (4.09)	5.66 (5.73)	159	280 (4.79); 236 (5.05) (sh); 210 (4.98)	3.70
$[Ni(dmophen)_2]^{2+}$	58.80 (59.90)	3.79 (3.84)	5.41 (5.38)	175	333 (4.79) (sh); 298 (4.97); 240 (5.07) (sh); 237 (5.17) (sh)	4.06
$[Ni(deophen)_2]^{2+}$	60.79 (61.22)	4.29 (4.37)	4.99 (5.10)	180	335 (4.66) (sh); 302 (4.82) (sh); 255 (4.87); 235 (4.92) (sh)	4.10
$[Ni(tphen)_2]^{2+}$	56.69 (57.16)	3.99 (3.51)	6.99 (7.02)	122	296 (4.43) (sh); 276 (4.95) 233 (5.11)	3.52
$[Ni(eophen)_2]^{2+}$	56.01) (55.96)	3.72 (3.73)	6.49 (6.53)	144	294 (4.20) (sh); 273 (4.89) 224 (5.01)	3.52
$[Ni(bpmp)(H_2O)_2]^{2+}$	38.32 (37.87)	3.25 (3.16)	13.16 (13.26)		792 (1.10); 532 (1.37); 327 (3.09); 296 (4.28) (sh); 277 (4.40)	
$[Mn(dmophen)_2]^{2+}$	51.01 (50.44)	3.21 (3.23)	4.78 (4.53)		331 (4.73); 296 (4.84); 276 (4.67)	
$[Mn(bpmp)(H_2O)_2]^{2+}$	37.01 (38.09)	3.31 (3.18)	12.48 (13.33)		329 (3.32); 297 (3.42) (sh); 285 (4.56)	

[a]Calculated values in parentheses.

molecules, but differ greatly from the IR spectra of the phenyl substituted phenanthroline complexes.

Conductance values in nitromethane recorded at room temperature for some of the nickel complexes with phenyl substituted ligands are in the range of 145 to 180 Ω^{-1} cm^2 mol^{-1}, indicating that the complexes are 1:2 electrolytes [16].

In the visible range of the electronic spectra, no electronic absorption bands are observed for any of the complexes except for the nickel complex of the bpmp ligand, where very weak transitions at 532 nm ($\epsilon = 23.4$ m^{-1} cm^{-1}) and 792 nm ($\epsilon = 12.5$ m^{-1} cm^{-1}) could be observed. This observation is consistent with the earlier statement that nickel(II) complexes generally undergo very little metal to ligand π backbonding [17, 18]. In the UV region there are spectral bands consistent with coordinated phen ligands, but the greater ϵ values for the phenyl substituted ligands are an indication of the softness of the phenanthroline ligands relative to the bpmp complexes, where in addition to phenanthroline (soft) there are two hard pyrazolyl moieties.

The susceptibility values for the phenyl substituted phenanthroline ligand complexes of nickel are in the range of 3.52 to 4.1 μ_B, which are in the expected range for high spin d^8 tetrahedral/pseudo-tetrahedral or octahedral/pseudo-octahedral complexes.

X-ray crystal structure of [Ni(dmophen)Cl$_2$]

The structure consists of monomeric [Ni(dmophen)Cl$_2$] complexes which are well separated from each other. There are two independent molecules in the cell, and a view of one complex is depicted in Fig. 1; selected bond lengths and angles in the structure are listed in Tables 4 and 5.

The complex adopts a four-coordinate geometry, the coordination being provided by two phen nitrogen atoms (N(1) and N(1a) for Ni(1); N(2) and N(2a) for Ni(2)) and by two chloride ions. In each case, the Ni atom lies on a crystallographic twofold axis that relates one

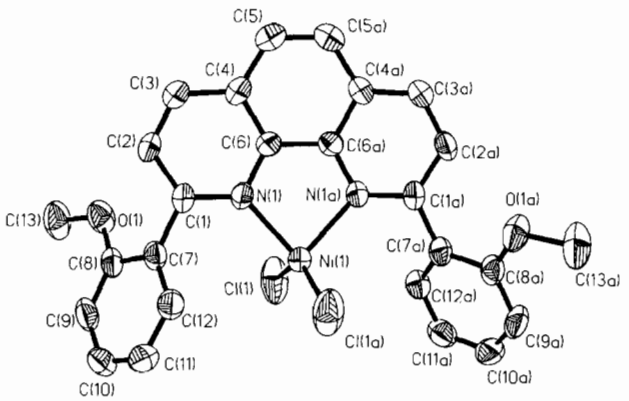

Fig. 1. View of the structure of the complex [Ni(dmophen)(Cl$_2$)]. The molecule centered on Ni(2) is essentially similar to the one shown here. Hydrogen atoms are omitted for clarity. Atoms labelled C(1a), etc. are related to atoms C(1), etc. by the crystallographic twofold axis running vertically in the Figure and passing through Ni(1) and the centers of the bonds C(6)–C(6a) and C(5)–C(5a).

TABLE 4. Selected bond lengths (Å) for $C_{26}H_{20}Cl_2N_2NiO_2$

Ni(1)–N(1)	2.016(4)	Ni(1)–Cl(1)	2.199(2)
Ni(1)–N(1A)	2.016(4)	N(1)–Cl(1A)	2.199(2)
Ni(2)–N(2)	2.013(4)	Ni(2)–Cl(2)	2.211(1)
Ni(2)–N(2A)	2.013(4)	Ni(2)–Cl(2A)	2.211(1)

TABLE 5. Selected bond angles (°) for $C_{26}H_{20}Cl_2N_2NiO_2$

N(1)–Ni(1)–Cl(1)	100.0(1)	N(1)–Ni(1)–N(1A)	83.4(2)
Cl(1)–Ni(1)–N(1A)	113.6(1)	N(1)–Ni(1)–Cl(1A)	113.6(1)
Cl(1)–Ni(1)–Cl(1A)	134.8(1)	N(1A)–Ni(1)–Cl(1A)	100.0(1)
N(2)–Ni(2)–Cl(2)	100.7(1)	N(2)–Ni(2)–N(2A)	82.9(2)
Cl(2)–Ni(2)–N(2A)	116.5(1)	N(2)–Ni(2)–Cl(2A)	116.5(1)
Cl(2)–Ni(2)–Cl(2A)	130.2(1)	N(2A)–Ni(2)–Cl(2A)	100.7(1)
Ni(1)–N(1)–C(1)	130.0(3)	Ni(1)–N(1)–C(6)	111.0(3)
Ni(2)–N(2)–C(14)	129.0(4)	Ni(2)–N(2)–C(19)	111.1(3)

half of the ligand to the other. The observed geometry is roughly tetrahedral, but owing to the constraints of the tetradentate ligand the bond angles around nickel do not approximate the idealized values. Thus, the N(1)–Ni(1)–N(1a) and N(2)–Ni(2)–N(2a) angles subtended by the phen moiety are 83.4(2) and 82.9(2)°, respectively, which are comparable to the values of 80.8(1)° in the six-coordinate $[Ni(bpmp)(H_2O)_2]^{2+}$ and 80.6(4)° in the five-coordinate $Ni(dpmp)Cl_2$ (where dpmp is 2-(3,5-dimethyl-*N*-pyrazolylmethyl)-9-methylethylether-1,10-phen) [1b], while the Cl(1)–Ni(1)–Cl(1a) and Cl(2)–Ni(2)–Cl(2a) angles are 134.8(1) and 130.2(1)°, respectively. The dihedral angles between the NiN(1)N(1a) and NiCl(1)Cl(1a) planes and their analogs at Ni(2) are 79.4 and 77.5°, respectively, close to the idealized value of 90°. The Ni(1)–N(1) and Ni(2)–N(2) interatomic distances of 2.016(4) and 2.013(4) Å, respectively, are shorter than the average values of 2.066 and 2.071 Å in the six-coordinate $[Ni(bpmp)(H_2O)_2]^{2+}$ and the five-coordinate $Ni(dpmp)Cl_2$, respectively [1b].

The phen and phenyl moieties are approximately planar, the largest deviation from the fourteen- and six-atom least-squares planes being 0.013 and 0.005 Å, respectively. As can be seen from Fig. 1, the dmophen ligand adopts a gauche conformation in the complex, the dihedral angles between the phen and phenyl planes associated with Ni(1) and those with Ni(2) being 51.5 and 50.4°, respectively, with the methoxy group rotated away from the metal. Bond lengths and angles in the ligand are unremarkable.

Electrochemistry

On the basis of the above spectroscopic, magnetic and crystallographic evidence we may deduce that the nickel and manganese complexes of the phenyl sub-

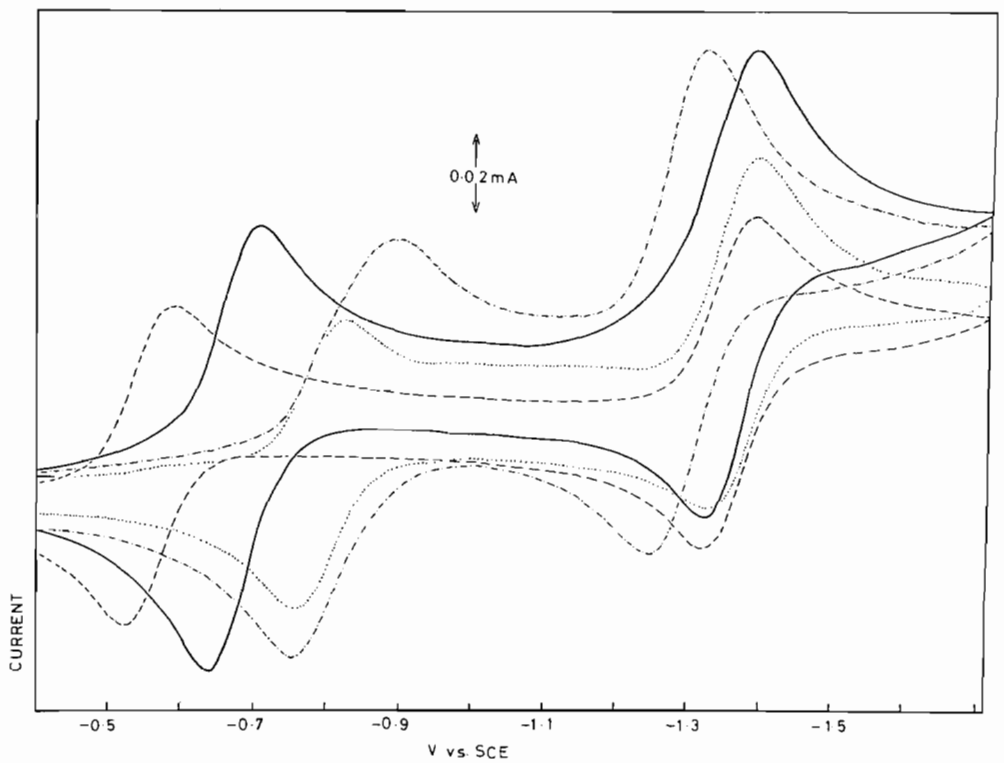

Fig. 2. Cyclic voltammograms for $[Ni(dmophen)_2]^{2+}$ (——), $[Ni(deophen)_2]^{2+}$ (– – –), $[Ni(tphen)_2]^{2+}$ (– · –) and $[Ni(eophen)_2]^{2+}$ (· · ·) in acetonitrile with 0.1 M TEAP as supporting electrolyte, scan rate 100 mV/s.

stituted phen ligands have pseudo-tetrahedral geometry, the particular topography being influenced by the presence of the bulky *ortho* substituents of the ligands. As is confirmed by earlier studies, steric interactions imposed by disubstituted ligands should be more than those of the monosubstituted systems. Consequently the nickel and manganese complexes of 2,9-di(*o*-substituted phenyl)-1,10-phen should be more distorted. This trend is reflected in the CV and DPV results. The electrochemical, cyclic voltammetry and differential pulse voltammetry studies were performed in acetonitrile. Both positive and negative potential ranges were examined. All the ligands are electrochemically inactive down to −1.90 V versus SCE. The CV profiles at various scan rates and at repeated scans were also investigated. Representative CV profiles of the nickel complexes are shown in Fig. 2, and the electrochemical data are presented in Tables 6 and 7.

The complex $[Ni(dtphen)]^{2+}$ exhibits two perfectly reversible one electron processes with $E_{1/2}$ values of +0.115 and −1.265 V, versus SCE, respectively, and with ΔE_p approximately 0.06 V for both redox couples. The complexes $[Ni(dmophen)_2]^{2+}$, $[Ni(deophen)_2]^{2+}$ and $[Ni(eophen)_2]^{2+}$ all also show two perfectly reversible one electron reduction processes, but the potentials are shifted to more negative values. The cathodic and anodic peak heights for the redox couples remain unchanged to various as well as to successive scan rates with $-i_c/i_a$ ratio of approximately 1. The complex $[Ni(tphen)_2]^{2+}$ also exhibits two redox couples in the negative potential range. The first redox couple is found to be quasi-reversible with ΔE_p values spreading from 0.12 to 0.14 V on increasing the scan rate from 0.02 to 0.10 V s^{-1}. The other redox couple is nearly reversible. By contrast, it was earlier reported that with 2,9-dimethyl-1,10-phen (dmp) or 2,9-di(*p*-methoxyphenyl)-1,10-phen (dap) no isolable complexes could be obtained, although $[Ni(dap)_2]^{2+}$ and (to a lesser extent) $[Ni(dmp)_2]^{2+}$ were sufficiently stable in CH_2Cl_2 and MeCN solutions to be studied by electrochemical methods [6]. It appears that steric effects provided by the *ortho* substituents of the phenyl moiety in the present

TABLE 6. Cyclic voltammetric and differential pulse voltammetric data for the M(II) ↔ M(I) redox couple[a]

Complex	Scan rate (V s^{-1})	CV					DPV	
		Cathodic E_p (V)	Anodic E_p (V)	ΔE_p (V)	$E_{1/2}$ (V)	$-i_c/i_a$	Cathodic E_p (V)	Anodic E_p (V)
$[Ni(dtphen)_2]^{2+}$	0.02	0.080	0.150	0.070	0.115	1.15	0.085	0.15
	0.05	0.090	0.150	0.060	0.120	1.07		
	0.10	0.090	0.150	0.060	0.120	1.18		
$[Ni(dmophen)_2]^{2+}$	0.02	−0.700	−0.635	0.065	−0.668	1.03	−0.70	−0.63
	0.05	−0.710	−0.645	0.065	−0.678	1.05		
	0.10	−0.710	−0.645	0.065	−0.678	1.06		
$[Ni(deophen)_2]^{2+}$	0.02	−0.590	−0.520	0.070	−0.555	1.08	−0.58	−0.51
	0.05	−0.585	−0.520	0.065	−0.553	1.06		
	0.10	−0.585	−0.550	0.065	−0.553	1.05		
$[Ni(tphen)_2]^{2+}$	0.02	−0.890	−0.770	0.120	−0.830	1.09	−0.89	−0.78
	0.05	−0.890	−0.760	0.130	−0.825	1.10		
	0.10	−0.890	−0.750	0.140	−0.820	1.08		
$[Ni(eophen)_2]^{2+}$	0.02	−0.820	−0.760	0.060	−0.790	1.06	−0.815	−0.745
	0.05	−0.820	−0.760	0.060	−0.790	1.04		
	0.10	−0.820	−0.750	0.070	−0.780	1.04		
$[Ni(bpmp)(H_2O)_2]^{2+}$	0.02	−0.380	−0.290	0.090	−0.335	1.44		
	0.05	−0.380	−0.280	0.100	−0.330	1.07		
	0.10	−0.430	−0.260	0.170	−0.345	0.89		
$[Mn(dmophen)_2]^{2+}$	0.02	−1.335	−1.275	0.060	−1.305	1.03	−1.330	−1.270
	0.05	−1.335	−1.275	0.060	−1.305	1.05		
	0.10	−1.345	−1.285	0.060	−1.315	1.09		
$[Mn(dmophen)_2]^{2+}$ [b]	0.10	−1.307	−1.213	0.100	−1.260			
$[Mn(bpmp)(H_2O)_2]^{2+}$ [b]	0.02	−0.92						
	0.05	−0.92	−0.83	0.110				
	0.10	−0.92	−0.82	0.100				

[a]Recorded in CH_3CN at 25 ± 1 °C with NEt_4ClO_4 as supporting electrolyte. HMDE working electrode, Pt wire auxiliary electrode and SCE reference electrode. [b]Glassy carbon working electrode and Ag/AgCl reference electrode.

TABLE 7. Cyclic voltammetric and differential pulse voltammetric data for M(I) ↔ M(0) redox couple[a]

Complex	Scan rate ($V\ s^{-1}$)	CV					DPV	
		Cathodic E_p (V)	Anodic E_p (V)	ΔE_p (V)	$E_{1/2}$ (V)	$-i_c/i_a$	Cathodic E_p (V)	Anodic E_p (V)
$[Ni(dtphen)_2]^{2+}$	0.02	−1.275	−1.215	0.06	−1.245	1.06	−1.265	−1.195
	0.05	−1.280	−1.210	0.07	−1.245	0.94		
	0.10	−1.275	−1.215	0.06	−1.245	0.96		
$[Ni(dmophen)_2]^{2+}$	0.02	−1.380	−1.320	0.06	−1.350	1.18	−1.375	−1.305
	0.05	−1.380	−1.320	0.06	−1.350	1.08		
	0.10	−1.380	−1.320	0.06	−1.350	1.08		
$[Ni(deophen)_2]^{2+}$	0.02	−1.375	−1.315	0.06	−1.345	1.04	−1.365	−1.300
	0.05	−1.375	−1.315	0.06	−1.345	1.04		
	0.10	−1.375	−1.315	0.06	−1.345	1.04		
$[Ni(tphen)_2]^{2+}$	0.02	−1.315	−1.235	0.08	−1.275	1.03	−1.300	−1.230
	0.05	−1.305	−1.235	0.07	−1.270	1.09		
	0.10	−1.310	−1.240	0.07	−1.275	1.06		
$[Ni(eophen)_2]^{2+}$	0.02	−1.380	−1.310	0.07	−1.345	1.06		
	0.05	−1.380	−1.320	0.06	−1.350	1.03		
	0.10	−1.380	−1.320	0.06	−1.350	1.13		
$[Mn(dmophen)_2]^{2+}$	0.02	−1.485	−1.425	0.06	−1.455	0.88	−1.470	−1.410
	0.05	−1.490	−1.430	0.06	−1.460	0.93		
	0.10	−1.490	−1.430	0.06	−1.460	0.95		
$[Mn(dmophen)_2]^{2+}$ [b]	0.10	−1.472	−1.372	0.10	−1.422			

[a]Experimental conditions: see footnote of Table 6.

ligands play an important role in stabilizing the complexes.

As shown in Fig. 3, in the case of $[Mn(dmophen)_2]^{2+}$ two perfectly reversible redox waves were observed over the hanging mercury drop electrode, at about −1.30 and −1.51 V versus SCE with ΔE_p 60 mV for both couples, while the same redox waves were observed to be quasi-reversible over glassy carbon electrode with $E_{1/2}$ values of −1.31 and −1.47 V, respectively, versus SCE* and with ΔE_p values of about 100 mV. The manganese complex of deophen showed a reduction potential at −1.42 V with a slight shoulder at −1.34 V and oxidation potential at −1.295 V with a slight shoulder at −1.375 V versus SCE. The first redox wave observed at the less negative potentials corresponds to the M(II) ↔ M(I) redox couple and the second redox wave observed at more negative potentials corresponds to the M(I) ↔ M(0) redox couple. The manganese complexes of dtphen, eophen and tphen do not exhibit any redox waves.

The redox behavior of the $[Ni(dmophen)_2]^{2+}$ and $[Ni(eophen)_2]^{2+}$ complexes can be compared to that of the nickel(II) catenates. The nickel(II) catenate obtained from interlocking catenands derived from dap

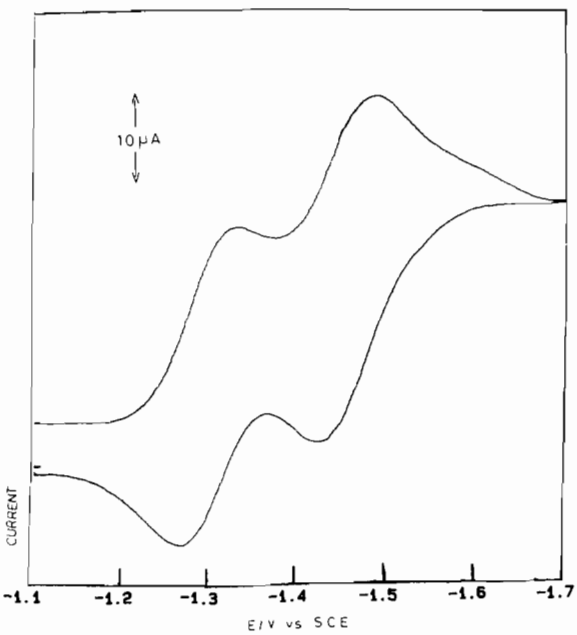

Fig. 3. Cyclic voltammogram for $[Mn(dmophen)_2]^{2+}$ in acetonitrile with 0.1 M TEAP as supporting electrolyte, scan rate 100 mV/s.

units have successive redox couples at $E_{1/2}$ values of −0.18 and −1.325 V versus SCE whereas the simple non-cyclic $[Ni(dap)_2]^{2+}$ complex exhibits two redox

*Calculated by applying the correction $E(Ag/AgCl) = E(SCE) + 0.045$ V [19].

waves with $E_{1/2}$ at -0.16 and -1.31 V versus SCE [20]. In these cases the redox processes have been well established to be Ni(II) ↔ Ni(I) and Ni(I) ↔ Ni(0) one electron transfers. It was noted that similarity of the $E_{1/2}$ values of the nickel(II) catenate and $[Ni(dap)_2]^{2+}$ complexes results from the topographical similarity of the two complexes. The slightly higher stability for the redox couple in nickel(II) catenate is accounted for by the topological effect of the interlocked rings. In the case of the $[Ni(dtphen)_2]^{2+}$ complex it can be seen from the data that the Ni(II) oxidation state is less stable (reduction occurs at less negative potentials) than both the nickel(II) catenate and its corresponding open analogue. The stability zone for the nickel(I) oxidation state, however, has increased and covers about 1.36 V, about 0.22 V more than in nickel catenate or $[Ni(dap)_2]^{2+}$. The reduction potential for Ni(0) has decreased by about 0.08 V when compared with the corresponding couple in nickel(II) catenate. However in case of $[Ni(dmophen)_2]^{2+}$ and $[Ni(deophen)_2]^{2+}$ the stability of nickel(II) has increased considerably and is about 0.5 and 0.37 V, respectively, greater than in nickel(II) catenate and about 0.52 and 0.39 V, respectively, greater than in $[Ni(dap)_2]^{2+}$. Although the stability zone for nickel(I) has evidently narrowed down, the nickel(I) oxidation state is electrochemically accessible and is quite stable. Moreover, the reduction potentials for this couple are slightly more negative than the corresponding peak observed for nickel(II) catenate.

The redox values for the Ni(II) ↔ Ni(I) couple observed in the cases of $[Ni(tphen)_2]^{2+}$ and $[Ni(eophen)_2]^{2+}$ show shifts towards more negative potentials of about -0.82 and -0.79 V versus SCE, respectively. This is attributable to the smaller distortion resulting from the absence of substitution at the 2 position of the phen ligands. The redox values are clearly reflective of the trend, that tetrahedral distortion leads to less negative potentials, a phenomenon observed earlier in the case of copper complexes [21]. Similar comparisons for the manganese complexes are precluded both because only $[Mn(dmophen)_2]^{2+}$ and $[Mn(deophen)_2]^{2+}$ exhibit electrochemical redox behavior and also because manganese complexes of the catenate and dap ligands have not been reported.

The electrochemical reversibility of the above nickel and manganese complexes can be contrasted to the behavior of complexes of bpmp. In complexes of copper(II) and nickel(II), and presumably with other metals, bpmp acts as a tetradentate ligand [1]; this explains the 1:1 metal:ligand ratio found here for Mn(II) (*vide supra*). The manganese complex of bpmp exhibits only one redox wave, with a large reduction wave at -0.97 V and a slight oxidation hump at -0.88 V versus SCE*, corresponding to the Mn(II) ↔ Mn(I) couple. The oxidation hump vanishes on successive scans. This is not surprising since monomeric manganese complexes are almost invariably electrochemically irreversible. However, the nickel complex of bpmp exhibits one quasi-reversible redox wave with a reduction potential at -0.43 V and oxidation potential at -0.34 V over glassy carbon versus SCE*, corresponding to the Ni(II) ↔ Ni(I) couple. No other peaks are observed.

It is fruitful to compare the electrochemical behavior of the present nickel complexes with that of $[Ni(bpy)_3]^{2+}$. In the latter, formal oxidation states of -1, 0, $+1$, $+2$ and $+3$ are accessible in MeCN, but the electrochemical behavior is complicated by a number of dissociative processes [22], and the Ni(III) ↔ Ni(II) couple is observed at 1.70 V versus SCE [23]. The absence of any oxidation (Ni(II) ↔ Ni(III) or Mn(II) ↔ Mn(III)) in the present studies results in part from the low coordination number (4) favored by these ligands, since this precludes the strong ligand field required for the stabilization of high oxidation states [24].

A comparison of CV and DPV results among large numbers of complexes of related ligands allows a distinction between metal localized or ligand localized electron transfer. Examination of the electrochemical data for the Fe, Co and Cu complexes of dtphen, dmophen, deophen, eophen, tphen, dap and catenate ligands [3, 20, 25] supports the conclusion that the first electron transfer (M(II) ↔ M(I)) is essentially metal localized; the potential range observed for this process spans the broad potential range from $+0.82$ to about -1.11 V versus SCE, and is metal dependent. In the case of a nickel complex of a quinquedentate macrocyclic ligand the couple is observed between -0.85 to -1.00 V versus SCE**, and the ESR spectrum of its reduced species demonstrates a metal localized reduction [5a]. Similar electrochemical and ESR results have been reported for the nickel complex of quinquepyridine [5c].

As can be seen from an examination of Fig. 4, the second electron transfer in the present set of complexes and the others noted above covers a very narrow range from -1.23 to -1.37 V versus SCE (i.e. a range of only 0.14 V), and the potentials are clearly more ligand dependent than metal dependent. This indicates that the electron transfer must be essentially ligand localized. The observation of essentially similar ΔE_p values of 60 to 70 mV in every case, irrespective of the metal, augments this argument. In fact the small potential range, which is about 13 kJ, demonstrates the similarity

*Calculated by applying the correction $E(Ag/AgCl) = E(SCE) + 0.045$ V [19].

**Calculated by applying the correction $E(Ag/AgCl) = E(Ag/Ag^+) + 0.35$ V [19].

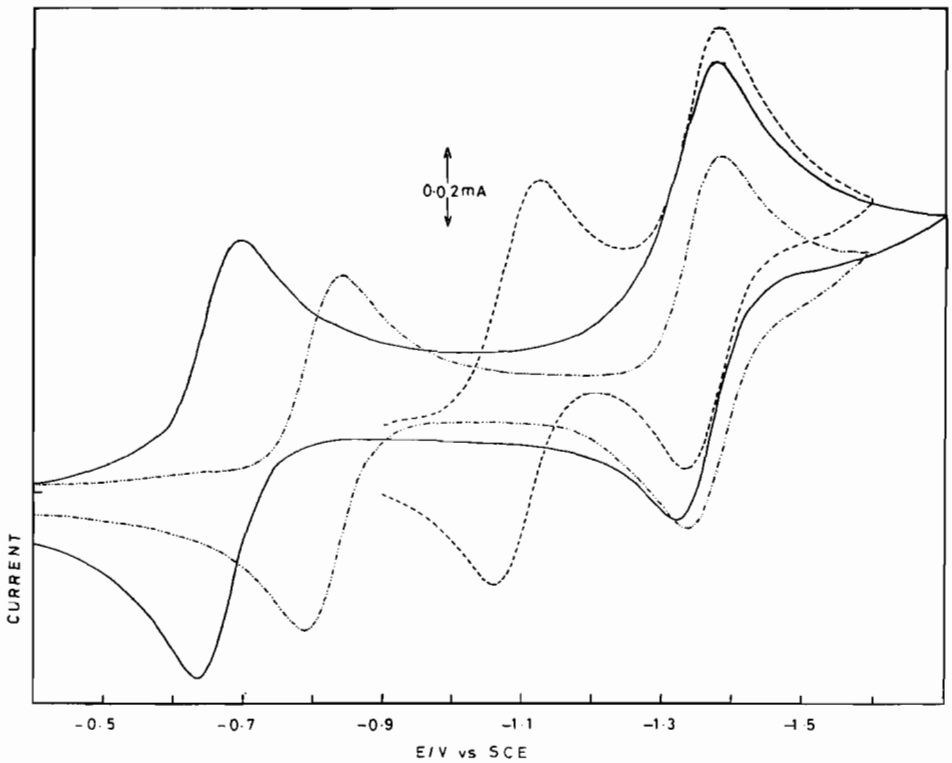

Fig. 4. Comparison of the cyclic voltammograms for $[Ni(dmophen)_2]^{2+}$ (——), $[Co(dmophen)_2]^{2+}$ (– · –) and $[Fe(dmophen)_2]^{2+}$ (– – –) with 0.1 M TEAP as supporting electrolytc, scan rate 100 mV/s. Data for the Co and Fe complexes from refs. 25 and 3, respectively.

of the ligand nature (soft π acceptors) in terms of electron accommodation even though the complexes vary in geometry and coordination number from four-coordinate distorted tetrahedral geometry in the present case to the helical quinquepyridine [5c], the pentagonal bipyramidal quinquedentate macrocyclic ligands [5a, 26] and the square planar macrocyclic ligands [27]. A survey of the literature of different types of geometrical complexes of various transition metals and soft ligands like bipyridine, terpyridine, phenanthroline [28] and their substituted analogues leads to the same conclusion. There are, however, a few cases where the reduction values span a wider range as in the case of the Cu(I) ↔ Cu(0) redox couple [1a], suggesting some metal involvement.

Although entirely definitive conclusions are precluded by the absence of ESR data, we may deduce from the electrochemical results that despite the lack of a macrocyclic environment or the topology of the catenands, the 2,9-di(*o*-substituted phenyl)-1,10-phen ligands are able to stabilize lower oxidation states, and that the *ortho* substituents on the phenyl groups influence the electrochemical properties of the complexes while the ligand binding to the reduced metal ion prevents its dissociation into free ligand and metal. Furthermore, we arc able to concludc with a degrce of confidencc that the first electron transfers are metal localized but that the second electron transfers are ligand localized.

Supplementary material

Tables S1 (hydrogen atom parameters), S2 (anisotropic thermal parameters) and S3 (listings of observed and calculated structure amplitudes) for the complex $[Ni(dmophen)Cl_2]$ are available from D.J.H. on request.

Acknowledgement

This work was supported by the National Science Foundation through Grant No. CHE-9007607 (to D.J.H.).

References

1 (a) Md. Athar Masood and D.J. Hodgson, *Inorg. Chem., 32* (1993) 4839; (b) *Inorg. Chem.*, in press.
2 (a) Md. Athar Masood and P.S. Zacharias, *J. Chem. Soc., Dalton Trans.*, (1991) 111; (b) *Transition Met. Chem., 17* (1992) 563.

3 Md. Athar Masood, R. Jagannathan and P.S. Zacharias, *J. Chem. Soc, Dalton Trans*, (1991) 2553; (b) Md. Athar Masood and P S Zacharias, *J Chem Soc., Chem Commun*, (1991) 152.

4 (a) D C. Olson and J. Vasilevskis, *Inorg Chem*, *8* (1969) 1611; (b) P.D. Rillema, J F. Endicott and E. Papaconstantinou, *Inorg Chem*, *8* (1969) 1611; (c) F.V. Lovecchio, E S. Gore and D H. Busch, *J Am Chem Soc*, *96* (1974) 3109

5 (a) C W.G Ansell, J. Lewis, P.R. Raithby, J.N. Ramsden and M. Schroder, *J Chem Soc, Chem. Commun*, (1982) 546; (b) E C. Constable, J. Lewis, M C. Liptrot, P.R. Raithby and M. Schroder, *Polyhedron, 2* (1983) 301; (c) E.C. Constable, M.D. Ward, M.G.B. Drew and G.A Forsyth, *Polyhedron, 8* (1989) 2551; (d) E.C. Constable, J Lewis and M. Schroder, *Polyhedron, 1* (1982) 311.

6 C.O. Dietrich-Buchecker, J.M. Kern and J.P. Sauvage, *J. Chem Soc., Chem Commun.*, (1985) 760.

7 K Nag and A. Chakravorty, *Coord Chem Rev*, *33* (1980) 87.

8 (a) D.G. Pillusbury and D.H. Busch, *J Am Chem. Soc., 98* (1978) 7836; (b) C.O. Dietrich-Buchecker and J P. Sauvage, *Chem Rev*, *87* (1987) 795; (c) *J Am Chem Soc*, *106* (1984) 3043.

9 P.A Goodson, A.R. Oki, J. Glerup and D.J Hodgson, *J Am Chem Soc., 112* (1990) 6248.

10 S.R. Cooper and M. Calvin, *J Am Chem. Soc*, *99* (1977) 6623.

11 K.J. Brewer, M. Calvin, R.S. Lumpkin, J.W. Otvos and L O. Spreer, *Inorg Chem*, *28* (1989) 4446.

12 P.A. Goodson, A.R. Oki and D.J. Hodgson, *Inorg Chim. Acta, 177* (1990) 59.

13 S. Mahaptra, D. Bhuniya and R. Mukherjee, *Polyhedron, 11* (1992) 2045.

14 A. Neves, S.M.D. Erthal, I Vencato, A.S. Ceccato, Y.P. Mascarenhas, O.R. Nascimento, M Horner and A.A. Batista, *Inorg Chem*, *31* (1992) 4749

15 (a) D L. Lewis, E.D Estes and D J Hodgson, *J Cryst Mol. Struct.*, (1975) 67, (b) W.R. McWhinnie and J.D. Miller, *Adv Inorg Chem Radiochem., 12* (1969) 135.

16 W.J. Geary, *Coord. Chem Rev*, *7* (1971) 81.

17 (a) A.B P Lever, G. Lawson and P.J. McChethy, *Can. J Chem*, *55* (1977) 3172; (b) R.J. Crutchlly and A.B.P Lever, *Inorg Chem*, *21* (1982) 22.

18 (a) M. Svoboda, H. Tom Dieck, C Kruger and Y.H.Z. Tsay, *Z Naturforsch, Teil B, 36* (1981) 814, (b) H. Tom Dieck, M Svoboda and T Z. Greiser, *Z Naturforsch, Teil B, 36* (1981) 823.

19 A.J. Bard and L.R. Faulkner, *Electrochemical Methods Fundamentals and Applications*, Wiley, New York, 1980, Fig E.1.

20 C.O. Dietrich-Buchecker, J.P. Sauvage and J M. Kern, *J. Am Chem. Soc*, *111* (1989) 7791.

21 R.D. Bereman, J.R. Dorfman, J. Bordner, D.P. Rillema, P. McCarthy and G.D. Shields, *J Inorg Biochem., 16* (1982) 47.

22 E.C Constable, *Adv Inorg Chem., 34* (1989) 1

23 (a) R. Prasad and B.D. Scaife, *J Electroanal. Chem*, *84* (1977) 37; (b) T. Saji and J. Aoyagui, *J. Electroanal Chem*, *58* (1975) 401.

24 F.A. Cotton and G. Wilkinson, *Advanced Inorganic Chemistry*, Wiley-Interscience, New York, 4th edn., 1980, pp 119–121.

25 Md. Athar Masood and P S Zacharias, *Polyhedron, 10* (1991) 811.

26 C.W.G. Ansell, J. Lewis, M.C Liptrot, P.R. Raithby and M Schroder, *J. Chem Soc, Dalton Trans.*, (1982) 1593.

27 R.R. Gagné and D.M. Ingle, *Inorg Chem*, *20* (1981) 420

28 D.E. Morris, K.W. Hanck and M.K. DeArmond, *J Am Chem Soc*, *105* (1983) 3032